Supplemental Document

Optics EXPRESS

Relationships between optical backscattering, particulate organic carbon, and phytoplankton carbon in the oligotrophic South China Sea basin: supplement

GUOQIANG QIU,[1] XIAOGANG XING,[2] EMMANUEL BOSS,[3] XIAO-HAI YAN,[1,4] RUI REN,[1] WUPENG XIAO,[1] AND HAILI WANG[1,*]

[1] *State Key Laboratory of Marine Environmental Science, Xiamen University, Xiamen 361102, China*
[2] *State Key Laboratory of Satellite Ocean Environment Dynamics, Second Institute of Oceanography, Ministry of Natural Resources, Hangzhou 310012, China*
[3] *School of Marine Sciences, University of Maine, 360 Aubert Hall, Orono, ME 04469, USA*
[4] *College of Earth, Ocean, and Environment, University of Delaware, Newark, DE 19716, USA*
[*] *hwang@xmu.edu.cn*

Supplement DOI: https://doi.org/10.6084/m9.figshare.14481435

Parent Article DOI: https://doi.org/10.1364/OE.422671

Relationships between optical backscattering, particulate organic carbon, and phytoplankton carbon in the oligotrophic South China Sea basin: supplemental document

GUOQIANG QIU,[1] XIAOGANG XING,[2] EMMANUEL BOSS,[3] XIAO-HAI YAN,[1,4] RUI REN,[1] WUPENG XIAO,[1] AND HAILI WANG[1,*]

[1]*State Key Laboratory of Marine Environmental Science, Xiamen University, Xiamen 361102, China*
[2]*State Key Laboratory of Satellite Ocean Environment Dynamics, Second Institute of Oceanography, Ministry of Natural Resources, Hangzhou 310012, China*
[3]*School of Marine Sciences, University of Maine, 360 Aubert Hall, Orono, Maine 04469, USA*
[4]*College of Earth, Ocean, and Environment, University of Delaware, Newark, DE 19716, USA*
**hwang@xmu.edu.cn*

Contents of this file:

1. Text S1. Uncertainty analysis of POC

The accuracy of POC measurement was based on several potential sources of errors [1,2]. Firstly, the carbon mass on the filters can be underestimated due to insufficient sampling of the rare large particles, incomplete retention of small particles, and breakage of the large particles. However, it is currently not possible for us to evaluate these. To mitigate these potential biases, a relatively large volume (4.3 L) of water was filtrated so as to include a larger number of rare particles, and a small vacuum pressure (<100 mm Hg) was adopted to increase the retention of the small particles and decrease the breakage of the large particles. Secondly, the carbon mass can be overestimated due to the adsorption of dissolved organic carbon (DOC) on the filters. To quantify this positive bias, each day a blank pre-combusted GF/F filter was placed on the filter manifold and wetted in 20 mL of 'pure' seawater for 1 hour so that it was saturated similarly to the POC samples. Here the 'pure' seawater refers to seawater filtered through a 0.22 µm Millipore cellulose acetate membrane. In this cruise, the measured carbon blank was 27.3±5.3 (mean ± standard deviation) µg C, with a range spanning 18.5-37.1 µg C (n=19). This result was comparable to previously published values, e.g., 21±9.4 µg C through *double filter blanks* approach, 18.9±10.6 µg C through *triple-volume intercept blanks* approach, and 25.4 µg C for the samples collected at 600 m [3], 48 µg C through *volume intercept blanks* approach [4]. Thus, carbon blanks represent a small uncertainty of 1.2 (5.3/4.3) mg m^{-3} of the final POC value.

2. Text S2. Backscattering correction

The accurate determination of b_b and b_{bp} was influenced by some factors including 1) the path length attenuation between instrument and detection volume, 2) the appropriate values of β_w and b_{bw}, and 3) the chosen value of parameter $\chi_p(140°)$.

Due to the path length attenuation, the measured backscattering was underestimated to some extent, and a compensated correction (sigma correction) was conducted following the 'User's Manual v2.8':

$$\beta=\sigma(K_{bb})\beta_u, \quad \text{(S1)}$$

$$\sigma(K_{bb})=k_1\exp(k_{exp}K_{bb}), \quad \text{(S2)}$$

where β_u is the uncorrected volume scattering function, k_1 and k_{exp} are constant parameters, and K_{bb} is the attenuation. K_{bb} was not measured in this cruise, and its value can be estimated empirically:

$$K_{bb}=a_p+a_g+0.4b_p, \quad \text{(S3)}$$

where a_p is the particulate absorption and was from the measured value (see Methods section). The a_g is the colored dissolved organic matter absorption and was estimated from a_{ph} empirically [5]:

$$a_g(\lambda)=0.2a_{ph}(\lambda)\exp(-0.014(\lambda\text{-}440)), \quad \text{(S4)}$$

where b_p is the particulate scattering and was estimated from the uncalibrated particulate backscattering (b_{bpu}):

$$b_p=b_{bpu}/\widetilde{b_{bp}}, \quad \text{(S5)}$$

where $\widetilde{b_{bp}}$ is backscattering probability and was set as 0.015. Fig. S1 shows that the calculated $\sigma(K_{bb})$ was very small (<1.015). Thus, in the SCS basin, the path attenuation had an insignificant impact on the β measurement.

Seawater scattering is generally very small and contributes <10% of the total scattering (b) even in the clear waters, but it contributes greatly to the total backscattering (b_b) owing to the nearly isotropic nature of water molecular scattering [6]. In the clearest water, the seawater backscattering (b_{bw}) can contribute 80% of b_b in the blue bands [7]. Therefore, accurately estimating b_{bw} is important for the final determination of b_{bp} and b_b. The measured or theoretical estimates of β_w and b_{bw} reported in previous studies show some difference [8-10]. Here two most widely-used estimates (Morel's and Zhang's approaches) were compared. In Morel's approach, β_w and b_{bw} can be estimated as follows:

$$\beta_w(\lambda,\theta)=2.18\cdot(\lambda/450)^{-4.32}\cdot[1+(1-\delta)/(1+\delta)\cos^2(\theta)]\cdot 10^{-4}, \quad \text{(S6)}$$

$$b_{bw}(\lambda)=3.5\cdot(\lambda/450)^{-4.32}\cdot 10^{-3}\cdot 0.5, \quad \text{(S7)}$$

where δ is the depolarization ratio, which value was set to 0.09 suggested by Morel [8]. In Zhang's approach, β_w and b_{bw} are estimated with dependencies on the measured temperature, salinity, and a depolarization ratio of 0.039. Fig. S2 shows the comparisons of these two approaches. In our observations, the variations of estimated $\beta_w(\lambda, 140°)$ from Zhang's approach were quite small (<2%), as the variations of temperature and salinity were also not large. The $\beta_w(\lambda,140°)$ from Zhang's approach were lower than the values from Morel's approach with the largest difference (15%) at 420 nm. In the SCS basin, the total backscattering was mainly contributed by seawater, and the contributions of $\beta_w(\lambda,140°)$ to $\beta(\lambda,140°)$ were up to 40-72% (Zhang's approach) and 43-82% (Morel's approach). Small difference in β_w estimates can cause a large difference in β_p estimates. Accordingly, the calculated $\beta_p(\lambda,140°)$ from Zhang's approach were significantly larger than the values from Morel's approach with the largest difference exceeding 60%. Zhang et al. [10] show that their results agreed with laboratory measurements [11,12] with an average difference of 1%. In this study, we therefore used Zhang's approach to estimate β_w and b_{bw}.

Theoretically, the best way to estimate b_{bp} is to integrate β_p over all the backward angles (90-180°). However, due to the difficulty in measuring β_p in the full backward hemisphere, the b_{bp} is practically estimated from β_p measured at a fixed angle (e.g. 140° for HS6). The conversion factor $\chi_p(140°)$ is not constant in the literature, and different values have been reported in many previous works, e.g. 1.18±0.041 from Boss and Pegau [13], 1.13 from Dana and Maffione [14], 1.21±0.062 from Chami et al. [15], and 1.167±0.049 from Sullivan and Twardowski [16]. These values are consistent to each other with a difference of only 7%. Thus, different $\chi_p(140°)$ could not induce a large difference in calculating b_{bp}. In this study we used the median of these values, 1.167 from Sullivan and Twardowski [16].

Figure S3 shows the final values of b_b and b_{bp}.

3. Text S3. Closure test of the optical measurements

The accuracy of the optical measurements was validated using a closure experiment. At two stations 'S2086' and 'S2097' (Fig. 1 in Introduction section), above-surface remote-sensing reflectance (R_{rs}) were measured with a Trios RAMSES-ACC/ARC meter following the above-water method [17]. Below-surface remote-sensing reflectance (r_{rs}) was computed from the measured R_{rs} [18]:

$$r_{rs}=R_{rs}/(0.52+1.7R_{rs}). \quad \text{(S8)}$$

Based on analyses and simulations of the radiative transfer equation, r_{rs} can be reconstructed from the IOPs (a and b_b), and with an error within 10% in clear waters [19]:

$$r_{rs}=0.0949u+0.0794u^2, \quad \text{(S9)}$$

$$u=b_b/(a+b_b)=(b_{bw}+b_{bp})/(a_w+a_p+a_g+b_{bw}+b_{bp}), \quad \text{(S10)}$$

where a_w is the seawater absorption which was estimated from the measurements of Pope and Fry [20], and a_g is the colored dissolved organic matter absorption and was estimated from a_{ph} empirically [5]. For a_p we used our own estimates (see Methods section). As shown in Fig. S4, r_{rs} estimated by these two methods were in good agreement, e.g. the differences were 5% and 2% at 470 nm, 24% and 21% at 510 nm, and both 0.5% at 700 nm, respectively. This closure experiment suggests that the *in-situ* optical measurements are of high quality.

4. Figures

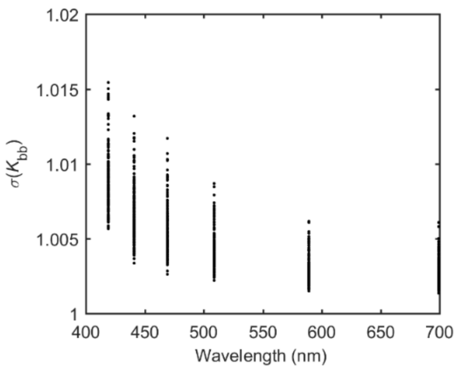

Fig. S1. The estimated $\sigma(K_{bb})$.

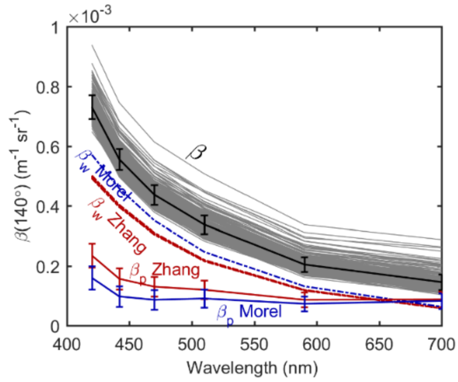

Fig. S2. The $\beta_w(\lambda, 140°)$ estimated from different models and the associated $\beta_p(\lambda, 140°)$. The grey lines show the measured total $\beta(\lambda, 140°)$, and the black line with bar shows its mean and standard deviation. The dashed blue and red lines show the $\beta_w(\lambda, 140°)$ estimated from Morel [8] and Zhang et al. [10], and the solid blue and red lines with bars show the associated mean β_p $(\lambda, 140°)$ with standard deviation.

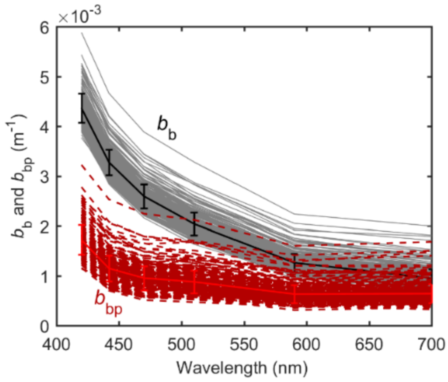

Fig. S3. Values of the total backscattering coefficient (b_b, gray lines) with their mean and standard deviation (black line and bar), and the particulate backscattering coefficient (b_{bp}, red dashed lines) with their mean and standard deviation (red line and bar).

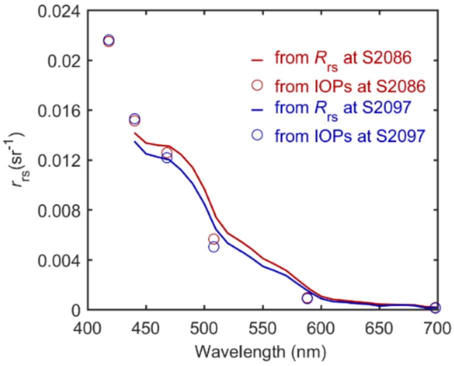

Fig. S4. Comparisons of the below-surface remote-sensing reflectance (r_{rs}) estimated from the measured above-surface remote-sensing reflectance (R_{rs}, lines) and the inherent optical properties (IOPs, circles) at the stations 'S2086' (red) and 'S2097' (blue).

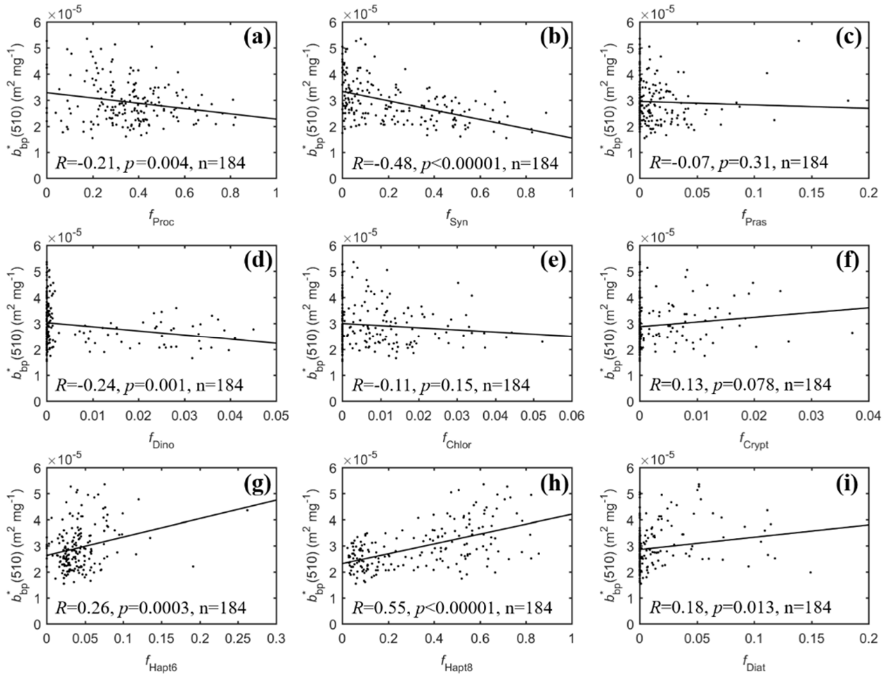

Fig. S5. Correlation coefficients between $b^*_{bp}(510)$ and the fraction to total Chla with phytoplankton group (a) *Prochlorococcus* (f_{Proc}), (b) *Synechococcus* (f_{Syn}), (c) Prasinophytes (f_{Pras}), (d) Dinoflagellates (f_{Dino}), (e) Chlorophytes (f_{Chlor}), (f) Cryptophytes (f_{Crypt}), (g) Haptophytes (Type 6) (f_{Hapt6}), (h) Haptophytes (Type 8) (f_{Hapt8}), and (i) Diatoms (f_{Diat}).

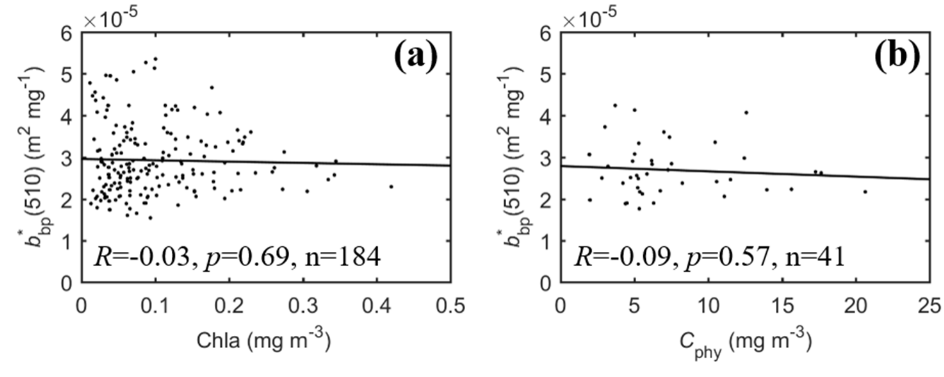

Fig. S6. Correlation coefficients between $b^*_{bp}(510)$ and (a) chlorophyll-a (Chla), (b) phytoplankton carbon (C_{phy}).

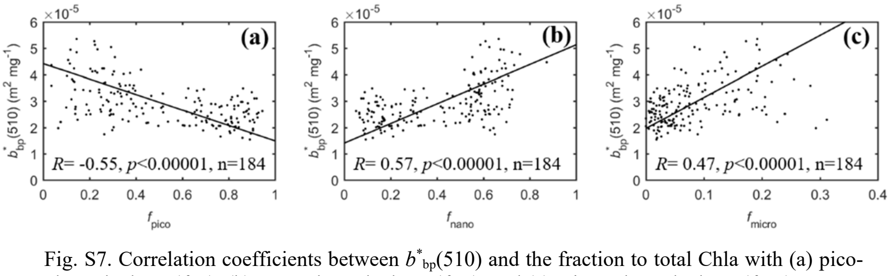

Fig. S7. Correlation coefficients between $b^*_{bp}(510)$ and the fraction to total Chla with (a) pico-phytoplankton (f_{pico}), (b) nano-phytoplankton (f_{nano}), and (c) micro-phytoplankton (f_{micro}).

References

1. D. Stramski, R. A. Reynolds, M. Babin, S. Kaczmarek, M. R. Lewis, R. Rottgers, A. Sciandra, M. Stramska, M. S. Twardowski, B. A. Franz, and H. Claustre, "Relationships between the surface concentration of particulate organic carbon and optical properties in the eastern South Pacific and eastern Atlantic Oceans," Biogeosciences **5**(1), 171-201 (2008).
2. W. D. Gardner, A. Mishonov, and M. J. Richardson, "Global POC concentrations from in-situ and satellite data," Deep Sea Res. Part II **53**(5-7), 718-740 (2006).
3. I. Cetinić, M. J. Perry, N. T. Briggs, E. Kallin, E. A. D'Asaro, and C. M. Lee, "Particulate organic carbon and inherent optical properties during 2008 North Atlantic Bloom Experiment," J. Geophys. Res.: Oceans **117**(C6), C06028 (2012).
4. S. B. Moran, M. A. Charette, S. M. Pike, and C. A. Wicklund, "Differences in seawater particulate organic carbon concentration in samples collected using small-and large-volume methods: the importance of DOC adsorption to the filter blank," Mar. Chem. **67**(1-2), 33-42 (1999).
5. A. Morel, "Light and marine photosynthesis: a spectral model with geochemical and climatological implications," Prog. Oceanogr. **26**(3), 263–306 (1991).
6. M. S. Twardowski, H. Claustre, S. A. Freeman, D. Stramski, and Y. Huot, "Optical backscattering properties of the 'clearest' natural waters," Biogeosciences **4**(6), 1041-1058 (2007).
7. A. Morel and B. Gentili, "Diffuse reflectance of oceanic waters: its dependence on Sun angle as influenced by the molecular scattering contribution," Appl. Opt. **30**(30), 4427-4438 (1991).
8. A. Morel, "Optical properties of pure water and pure sea water," in *Optical Aspects of Oceanography*, N. G. Jerlov, and E. S. Nielsen, eds. (Academic Press, New York, 1974), pp. 1-24.
9. H. Buiteveld, J. H. M. Hakvoort, and M. Donze, "The optical properties of pure water," Proc. SPIE **2258**, 174-183 (1994).
10. X. Zhang, L. Hu, and M.-X. He, "Scattering by pure seawater: Effect of salinity," Opt. Express **17**(7), 5698-5710 (2009).
11. A. Morel, "Etude Experimentale de la diffusion de la lumiere par l'eau, les solutions de chlorure de sodium et l'eau de mer optiquement pures," Journal de Chimie Physique **10**, 1359-1366 (1966).
12. A. Morel, "Note au sujet des constantes de diffusion de la lumiere pour l'eau et l'eau de mer optiquement pures," Cahiers Oceanographiques **20**, 157-162 (1968).
13. E. Boss and W. S. Pegau, "Relationship of light scattering at an angle in the backward direction to the backscattering coefficient," Appl. Opt. **40**, 5503-5507 (2001).
14. D. R. Dana and R. A. Maffione, "Determining the Backward Scattering Coefficient with Fixed-Angle Backscattering Sensors–Revisited," in *Ocean Optics XVI Conference* (2002).
15. M. Chami, E. Marken, J. J. Stamnes, G. Khomenko, and G. Korotaev, "Variability of the relationship between the particulate backscattering coefficient and the volume scattering function measured at fixed angles," J. Geophys. Res.: Oceans **111**, C05013 (2006).
16. J. M. Sullivan and M. S. Twardowski, "Angular shape of the oceanic particulate volume scattering function in the backward direction," Appl. Opt. **48**(35), 6811-6819 (2009).
17. J. L. Mueller, C. Davis, R. Arnone, R. Frouin, K. Carder, Z. Lee, R. Steward, S. Hooker, C. D. Mobley, and S. McLean, "Above-water radiance and remote sensing reflectance measurements and analysis protocols," in *Ocean Optics Protocols for Satellite Ocean Color Sensor Validation* (NASA, 2000), pp. 98-107.
18. Z. Lee, K. L. Carder, and R. A. Arnone, "Deriving inherent optical properties from water color: a multiband quasi-analytical algorithm for optically deep waters," Appl. Opt. **41**(27), 5755-5772 (2002).
19. H. R. Gordon, O. B. Brown, R. H. Evans, J. W. Brown, R. C. Smith, K. S. Baker, and D. K. Clark, "A semianalytic radiance model of ocean color," J. Geophys. Res.: Atmos. **93**(D9), 10909-10924 (1988).
20. R. M. Pope and E. S. Fry, "Absorption spectrum (380–700 nm) of pure water. II. Integrating cavity measurements," Appl. Opt. **36**(33), 8710-8723 (1997).